Geophysical Research Letters

RESEARCH LETTER
10.1029/2020GL087014

Interannual Variability of the Outflow of Weddell Sea Bottom Water

Arnold L. Gordon[1], **Bruce A. Huber**[1], **and E. Povl Abrahamsen**[2]

[1]Lamont-Doherty Earth Observatory, Columbia University, Palisades, NY, USA, [2]British Antarctic Survey, Natural Environment Research Council, Cambridge, UK

Key Points:
- The two-decade time series of Weddell Sea Bottom Water (WSBW) export recorded a marked reduction of salinity to 34.615 in early 2016
- The WSBW low salinity was due to increased upper layer water injection at the V-shaped trough within the shelf/slope regime
- The fresher WSBW is induced by increased cyclonic Weddell Gyre wind stress curl deepening of the V-shaped trough, aided by thermobaricity

Supporting Information:
- Supporting Information S1

Correspondence to:
A. L. Gordon, agordon@ldeo.columbia.edu

Citation:
Gordon, A. L., Huber, B. A., & Abrahamsen, E. P. (2020). Interannual variability of the outflow of Weddell Sea Bottom Water. *Geophysical Research Letters*, *47*, e2020GL087014. https://doi.org/10.1029/2020GL087014

Received 8 JAN 2020
Accepted 13 FEB 2020
Accepted article online 18 FEB 2020

Abstract The Weddell Sea Bottom Water (WSBW) export from 1999 to 2019 displays distinct seasonal and interannual variability. From 2014 into 2017 a marked salinity decrease was recorded, with the lowest salinity, 34.615, attained in early 2016. The reduced salinity is derived from the V-shaped trough formed by a double front along the shelf break of the Weddell Gyre's western boundary, which is filled with a blend of surface water and modified Weddell Deep Water. We estimate that when the V-shaped apex attains a depth of greater than ~700 m, the thermobaric effect promotes its descent into the WSBW. We propose that this occurred during anomalously strong cyclonic wind stress curl over the Weddell Gyre from 2014 into 2017, which increased the intensity of the gyre and its western boundary current, deepening the V-shape trough. The WSBW salinity increased to its prior to 2014 values as the wind stress relaxed in 2018.

Plain Language Summary The Weddell Sea Bottom Water (WSBW) emanating from the western Weddell Sea impacts the characteristics of the Antarctic Bottom Water that ventilates the deep ocean. From 2014 to 2017 the WSBW attained its lowest salinity values since we began monitoring the outflow in 1999. We present evidence that the change was a consequence of a wind-induced spin-up of the Weddell Gyre, which increased intensity of the western boundary current of the Weddell Sea enabled relatively low salinity winter surface layer water to descend into the bottom layer, through the thermobaric effect. Since 2017 the salinity of the WSBW returned to the long-term average, as the wind stress forcing relaxed.

1. Introduction

The Southern Ocean circulation is far from zonally symmetric, since the Antarctic Circumpolar Current (ACC) shifts in latitude in response to the wind patterns and to sea floor morphology, as it encircles Antarctica. Poleward of the ACC is the Antarctic zone, with a cold/fresh surface layer (Antarctic Surface Water, AASW) over warmer/saltier deep water; and still further south is the continental margin of Antarctica, where dense shelf water forms, at freezing point temperature (~ −1.9 °C). The ACC northward displacement is greatest in the Atlantic Ocean sector, which enables the development of the large cyclonic Weddell Gyre, driven by the wind stress curl induced by the westerlies near the ACC and the easterlies along the Antarctic margin (Vernet et al., 2019). At various sites along margins of Antarctica dense shelf water feeds into the Antarctic Bottom Water (AABW) spreading into the world ocean (Legg et al., 2009; Orsi et al., 1999, 2001, 2002; Purkey & Johnson, 2013; Purkey et al., 2018; Stewart & Thompson, 2013).

Relatively warm, salty Circumpolar Deep Water of the ACC enters the eastern limb of the Weddell Gyre, forming Weddell Deep Water (WDW), capped by the AASW. Through various pathways the WDW feeds into the formation of dense precursors of AABW along the continental margins of the Weddell Sea through processes including heat and freshwater exchange with the atmosphere and ice shelves. The densest Weddell Sea component of AABW is referred to as Weddell Sea Bottom Water (WSBW), generally identified as water colder than $\theta = -0.7$ °C (Carmack & Foster, 1975).

The Western Boundary Current (WBC) of the Weddell Gyre advects WSBW northward to eventually feed into the global spread of AABW marking the lower cell of the global overturning circulation (Gordon et al., 1993; Marshall & Speer, 2012; Muench & Gordon, 1995). The site M_3 in the northwestern sector of the Weddell Gyre, south of the South Orkney Plateau, falls within the stream of WSBW (Figure 1, Gordon et al., 2001; Gordon et al., 2010). The M_3 time series provides a unique time series, extending over the 20

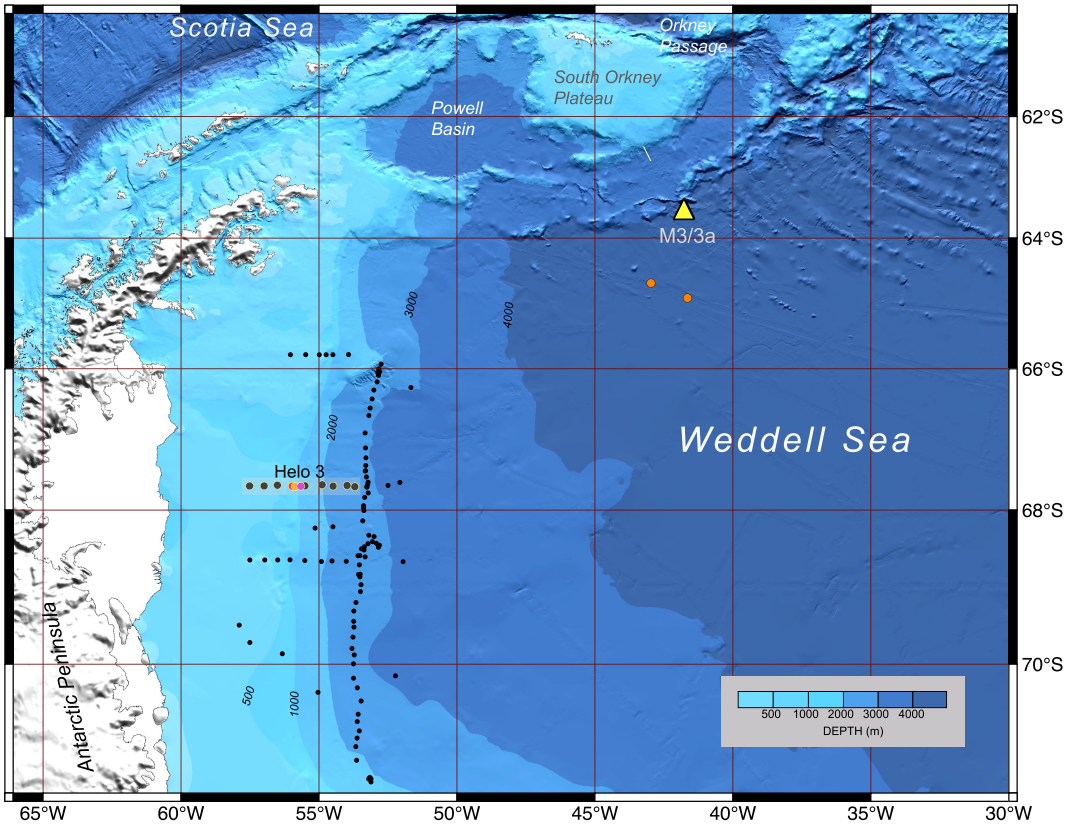

Figure 1. Map of the location of the M_3/M_{3a} moorings (nominal depth 4,500 m; M_3 and M_{3a} are separated by 2 km), plus the CTD helicopter stations obtained from the 1992 Ice Station Weddell (Gordon et al., 1993, the zonally oriented dots) and from the ice floe (the meridionally oriented dots). Helo section 3 is highlighted, with stations 23, 28, and 29 across the shelf-slope front as colored dots corresponding to the traces in Figure 3a. Two CTD stations from 2008 POLARSTERN expedition ANT XXIV/3 (202-1, depth 4773 m; 204-2 4678 m) used in Figure 2 are indicated as orange dots. Bathymetry, coastline, and ice shelf outlines are from the International Bathymetric Chart of the Southern Ocean (IBCSO; Arndt et al., 2013).

year period from February 1999 to January 2019 (Figure 2). The 2007–2008 gap, due to mooring recovery failure, reduces the time series to 18 years. The time series captures a marked decrease in WSBW salinity in 2014 into 2017, with recovery in 2018. The objective of our study is to describe this recent freshening and investigate possible causes.

2. Data

An array of oceanographic moorings south of the South Orkney Plateau has been recovered and redeployed approximately every 2 years since 1999. Since 2005 this has been performed under the auspices of a Memorandum of Understanding between Lamont-Doherty Earth Observatory of Columbia University and the British Antarctic Survey. The most recent rotation was carried out in January 2019. Only temperature-salinity (T/S) data from mooring M_3 is presented here. Details of the mooring configuration and data are given in the supporting information. Additional T/S data from conductivity-temperature-depth (CTD) profiles in the vicinity of M_3 and along the eastern Antarctic Peninsula are used in the analysis. CTD data sources are detailed in the supporting information Table S1.

3. Results

3.1. WSBW Time Series

The time series of the bottom water characteristics at mooring M_3 (Figure 2a) reveals a distinct seasonal cycle in both potential temperature and salinity, a consequence of the seasonality of the northward wind, along the eastern continental margin of the Antarctic Peninsula, as discussed by Gordon et al., 2010. The coldest

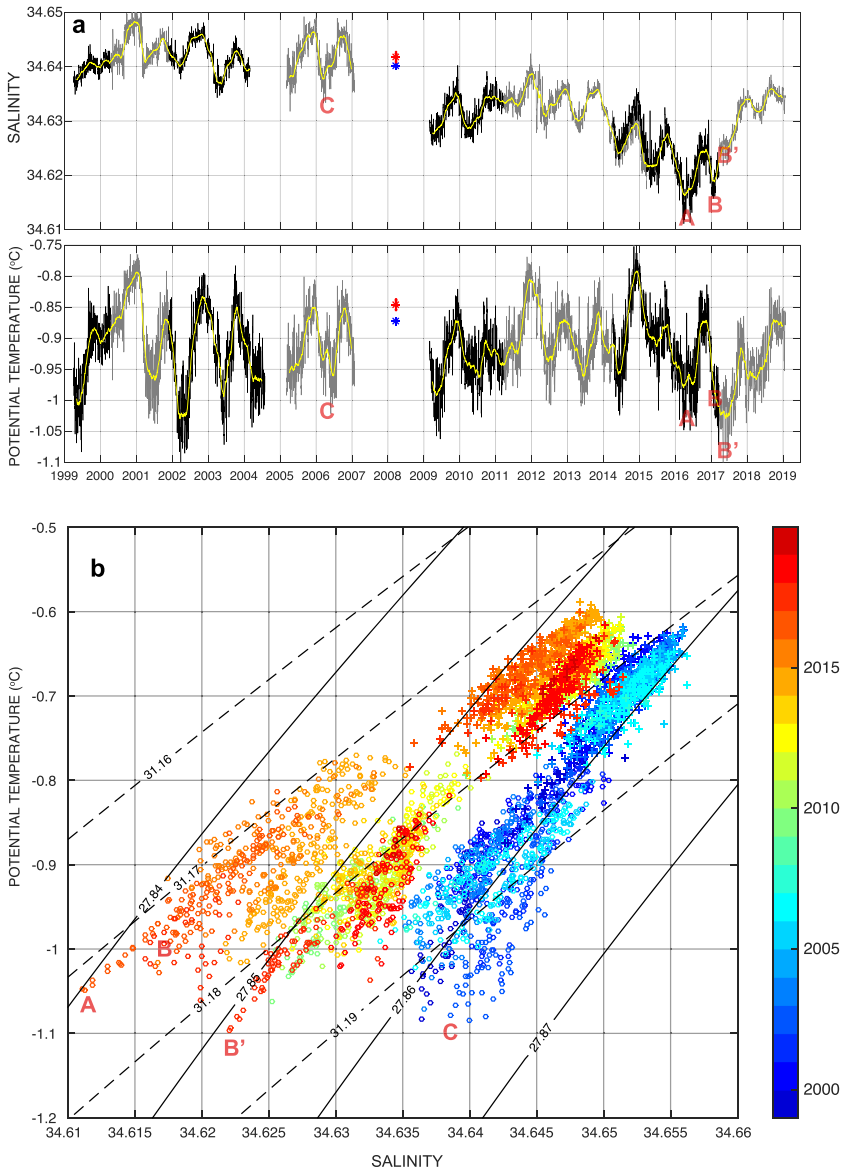

Figure 2. a. Mooring M_3 potential temperature and salinity time series (Figure 2a) 20 m above the seafloor. Individual mooring deployments are alternately shaded dark and light. The positions of the 2016 and 2017 "fresh" and "cold" events are marked, respectively, with A, B, and B′ as are the cold events before 2007, as exemplified by C. The yellow lines are 60-day running means. Data from two CTD profiles upstream from M_3 obtained in late March 2008 (see Figure 1) are displayed as blue and red symbols. The plotted data are the deepest 10 m sampled from station 202-1 (blue) and 204-2 (red). Metadata and online sources for the two profiles are given in the supporting information Table S1. b. The M_3 T/S scatter, color coded by year, for the bottom sensor shown in Figure 2a (o), and for the T/S sensors at 470 m above the seafloor (+). The T/S positions of the "fresh" and "cold" events A, B, B′, and C are marked. Potential density isopycnals are shown for reference pressures of 0 (σ_0, solid); 700 dbar ($\sigma_{0.7}$, dashed).

bottom water at M_3 occurs in the austral fall season (April–June), indicating that the export of relatively cold, dense shelf water is strongest in the previous summer season, the ~3 month delay reflecting the mean bottom velocity at M_3 of 0.1 m s^{-1} (Gordon et al., 2010). The summer export of shelf water is induced by weakening northward wind and associated westward Ekman transport, which enables a seaward shift in the shelf/slope front, permitting the export of dense shelf water onto the continental slope and into the WSBW stream; whereas the stronger winds in winter shift the front shoreward, limiting shelf water access to the slope (Gordon et al., 2010). There are also interannual changes of the wind and export of shelf

water, which can be attributed to coupling with more global-scale climate features, that is, El Niño–Southern Oscillation (ENSO, Gordon et al., 2010; McKee et al., 2011).

A T/S view of the bottom water at M_3 (Figure 2b) reveals a "fan-shaped" triangle form in T/S space, with the cold water component, observed by the sensors 20 m above the sea floor, along the base of the triangle, exhibiting a salinity range of 0.03; whereas the salinity range at 470 m above the sea floor, marking the top of the T/S triangle, is 0.01. Attenuation of the salinity span with distance off the sea floor is a consequence of the bottom-intensified characteristics of the density-driven gravity current origin of the benthic plume (Gordon et al., 2010; Legg et al., 2009). The seasonal signal is also attenuated with distance from the bottom (supporting information Figure S2).

During the period from 2014 into 2017 there is a shift toward a less saline WSBW, with the lowest WSBW salinity, of 34.615, occurring in the austral summer/fall 2016 (marked as A in Figures 2a and 2b). In the austral summer 2017 another low salinity event is recorded (B in Figure 2a) of approximately 34.62, which was followed about 2 months later by colder water, about −1.1 °C (marked as B′ in Figures 2a and 2b). Before 2007 the cold events were of higher salinity, ~34.64 (marked as C in Figures 2a and 2b). Gordon et al. (2010) and McKee et al. (2011) attribute the cold, relatively salinity 2002 event to strong northward wind in the southwest Weddell Sea in the vicinity of the coastal polynya off the Ronne Ice Shelf, a site of generation of cold high salinity shelf water, which eventually was exported to the deep ocean. It is noted that the salinity associated with B′ (Figure 2a) is salty relative to the B event and likely incorporates greater amounts of high salinity shelf water from the Ronne region. In this study we focus on the low salinity events marked by A and B, which we believe are a consequence of increased Weddell Gyre WBC, as described below. We speculate that the B′ event is drawn from the southwest Weddell Sea, and is also a response to the wind, with the 2 month delay relative to B induced by the additional advective path.

The M_3 time series T/S scatter diagram (Figure 2b) reveals a temporal shifting toward lower salinity WSBW. The total drop in WSBW salinity, of ~ 0.03, occurs mainly in two jumps: a smaller offset, 0.005, in 2007–2009 and a larger change, 0.015, occurring from 2014 into 2016, the remaining 0.01 drop more smoothly spread out over the time series. In 2018 the WSBW salinity rebounds to the 34.63 characteristic of values prior to 2014. The 2007–2009 smaller drop occurred during the unfortunate gap in the time series. However, CTD stations in the austral summer 2008 near the M_3 site (Figure 2a) suggest that the salinity drop mainly occurred in 2008–2009.

The Ice Station Weddell (ISW) helicopter section 3 (Figures 1 and 3b; Gordon, 1998) traversed the deep water to shelf water regimes. A sharp front (often referred to as the Antarctic Slope Front, e.g., see Jacobs, 1991) is observed (Figure 3b) in the temperature section near the shelf break, which coincides with a narrow zone of relatively low salinity water, forming a V-shaped trough extending to 700 m. Gill (1973) states "At the edge of the shelf in the western Weddell Sea, there is a V-shaped double front, above which lies the cold freshwater from the coastal current. The descending cold salty water from the shelf meets the warmer fresher water of the open ocean pycnocline at the base of the V and the two waters mix to form bottom water which then runs down the continental slope."

Landward of the shelf break is the freezing point shelf water with salinity above 34.6, above which is the warmer modified WDW (mWDW), drawn from WDW of the Weddell Sea. The pycnocline separates the WDW from the AASW, which slopes to greater depth as the continental margin is approached, associated with the northward geostrophic WBC of the Weddell Gyre.

We propose that the reduced salinity of WSBW observed in 2015–2017 is caused by a deepening of the apex of the V-shaped trough, along with the thermobaric effect, enabling the increased injection of the relatively low salinity, thus leading to fresher WSBW.

The CTD stations 23 and 28 on the inshore side of the V-shaped trough capture the mWDW, which is colder than −1.0 °C with salinity of less than 34.60. Increased injection of this water type can account for the observed freshening of the WSBW in 2014–2017. It is possible that a simple 2-point, linear mixing line (dashed black line on Figure 3a) of the lower WDW with CTD station 23 T/S point <−1.5 °C and 34.55, with a $\sigma_{0.7}$ of 31.17 (marked by * on Figure 3a), can explain the WSBW marked by A (Figure 2). Additionally, increased injection of mWDW into the mixture of mWDW with shelf water can provide the cold end-

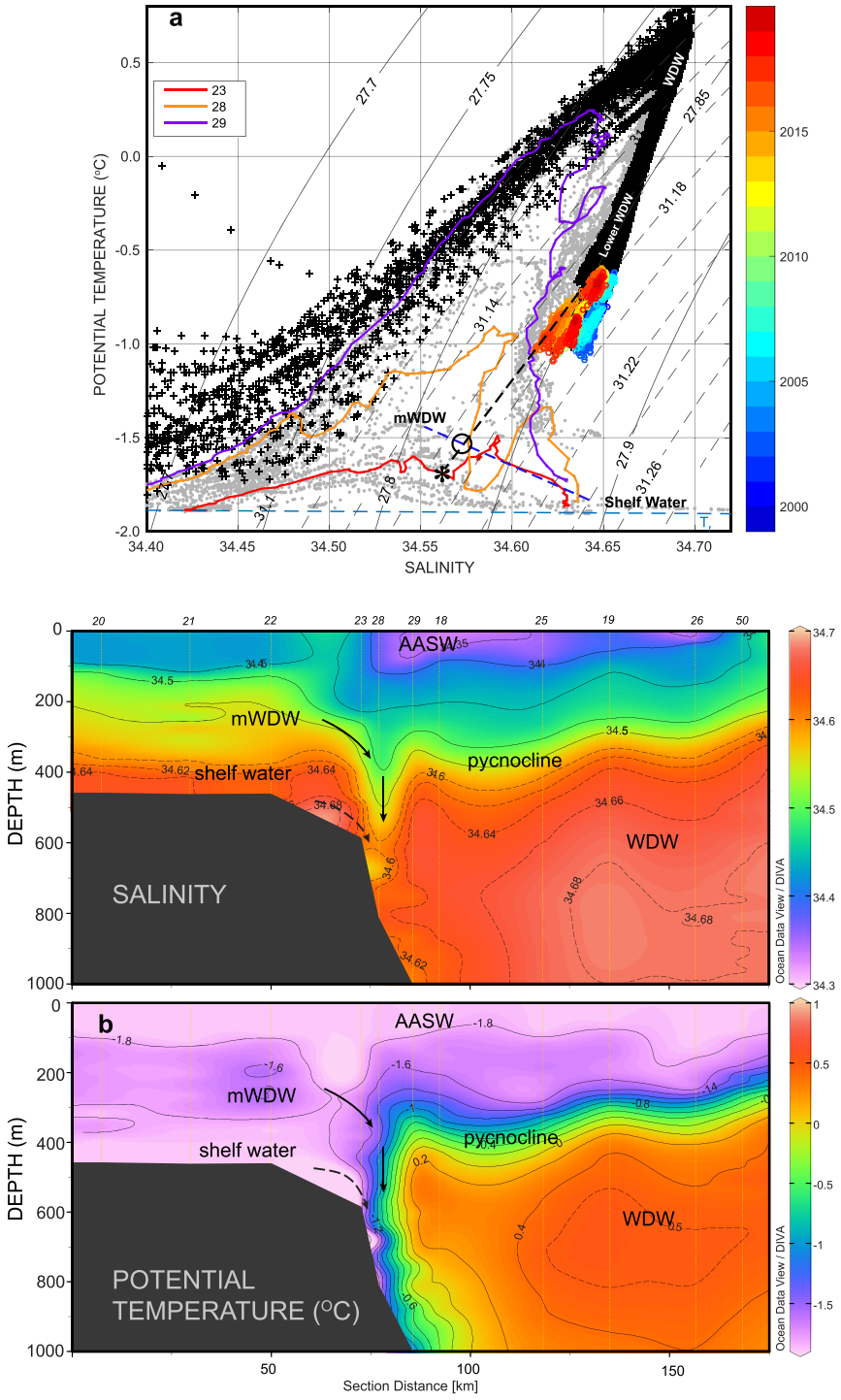

Figure 3. a. T/S scatter from M_3, color coded by year, with the CTD stations obtained from the Ice Station Weddell (ISW) and ship-based CTD near the M_3 mooring. The σ_0 and $\sigma_{0.7}$ potential density contours are shown by the solid and dashed gray lines, respectively. The CTD stations 23, 28, and 29 within the V-shaped trough observed by the ISW helicopter section (Figure 3b) are shown by the color lines. The cold end-member, marked by X, for the low salinity WSBW of 2016 from a simple two end-member linear mixing defined by the black dashed line; alternatively the cold end-member, marked by O symbol, may be a mixture of mWDW and shelf water along the blue dashed line. b. ISW CTD from Helicopter section 3 along 67°40′S (see Figure 1) obtained in 4–12 May 1992. The low salinity V-shaped trough falls along the thermal front separating the shelf from the open ocean stratification from the shelf regime. The arrows denote the descent of the upper layer waters and mWDW into the V-shaped trough that can further descend to the WSBW if enabled by the thermobaric effect. The dashed arrow marks the export path for the high salinity shelf water.

member, as discussed in the WSBW bottom water recipe presented by Foster and Carmack (1976) (dashed blue line in Figure 3a).

Descent of the cold water filling the V-shaped trough is subject to greater compression, the thermobaric effect, and has the potential to reach into the WSBW. The critical density may be reached by salinity increase within the V-shaped trough and/or deepening of the apex of the V-shaped trough. Based on the required cold end-member water for the 2016 WSBW T/S and the 31.17 $\sigma_{0.7}$ isopycnal (Figures 2 and 3), we estimate that this critical depth is about 700 m. We next consider regional-scale factors that might drive the increased contribution of V-shaped trough water and the resultant freshening of the WSBW.

3.2. Weddell Gyre and WBC Spin-Up

The Weddell Gyre, between the ACC near 50°S in the Atlantic sector, and the margins of Antarctica, is the largest of the cyclonic gyres of the South Ocean. It is driven by cyclonic wind stress curl between the westerlies and the polar easterlies (Armitage et al., 2018). The wind stress curl anomaly, computed from the ERA-Interim reanalysis (Dee et al., 2011, Figure 4), displays strong interannual variability, which would be mirrored by the Weddell Gyre intensity (Armitage et al., 2018, their Figure 6). Beginning in 2014 the wind stress curl anomaly shifts to more cyclonic state, peaking at the latter half of 2015, recovering in 2016, returning to long-term mean values in late 2017 into 2018. Cyclonic forcing also attains a maximum value in the late 1990s, albeit less extreme than the 2015–2016 event.

We suggest the following sequence to explain the 2015–2016 WSBW freshening (0.015): (1) wind-induced spin-up of the Weddell Gyre; (2) increased northward transport of the Weddell Gyre WBC; (3) deepening of the V-shaped trough; and (4) as the apex deepens, the thermobaric effect triggers descent of the cold, lower salinity water into the WSBW. We note that the rate of change of the 2007–2010 wind stress curl anomaly marks the second largest prolonged shift toward a more cyclonic state, surpassed by the much larger 2014–2016 spin-up (Figure 4). We speculate that it may have induced the 2007–2009 WSBW salinity reduction (~0.005).

ENSO and the Southern Annular Mode (SAM) affect the atmospheric forcing of the Southern Ocean (Fusco et al., 2018; Meijers et al., 2019; Yuan, 2004; Yuan et al., 2018). The relationship of nino3.4 and SAM to the wind stress curl anomaly over the Weddell Gyre (Figure 4) indicates strong cyclonic wind stress curl is more common during +SAM when the westerlies are stronger and shifted poleward, but an ENSO role is also likely, as the most extreme cyclonic wind stress curl anomaly of -5×10^{-8} N m^{-3} characteristic of the 2015–2016 event occurred when SAM and nino3.4 were both strong and in-phase, unlike conditions in the late 1990s when the +SAM followed the El Niño by 2 years (Figure 4). Positive wind stress curl anomaly is common when SAM is less than +0.5, without an obvious ENSO role.

We find that the peak cyclonic wind stress curl of late 2015 (Figure 4) was followed by the low WSBW salinity event in austral fall 2016. However, the lag of the WSBW low salinity event to the time when the wind stress curl attained values greater than the 1996–1999 maximum (Figure 4) is ~18 months. Noting the ~3 month time lag between the Weddell Sea western boundary WSBW production to its arrival at M_3 (Gordon et al., 2010), we suggest that the lag between the wind stress curl forcing and the Weddell Gyre WBC spin-up (and V-shaped trough intensification) is approximately 15 months or better stated as slightly longer than 1 year.

Meijers et al. (2016), using archived observations of the continental slope near the tip of the Antarctic Peninsula, where a branch of the WBC of the Weddell Gyre turns westward, find periods of stronger westward current, between 600 and 2,000 m. The density of the slope current is decreased as eastward wind stress over the northern Weddell Sea increases, with a lag of 6–13 months, which may be indicative of the response time of the Weddell Gyre to wind stress changes. Armitage et al. (2018) find a rapid response of the sea level anomaly in the Weddell Gyre to the wind curl (see their Figure 6b). Su et al. (2014) present a highly idealized model to investigate the response of the Weddell Gyre isopycnal depths along the side-wall boundaries to the seasonal wind stress forcing. They find 5 months lag between the wind stress maximum and the deepening of the isopycnals at the boundaries of the Weddell Gyre.

Besides the impact on the WSBW, which is the focus of this study, there are other anomalies in the Weddell region in the same time frame that may also be a response to the Weddell Gyre spin-up.

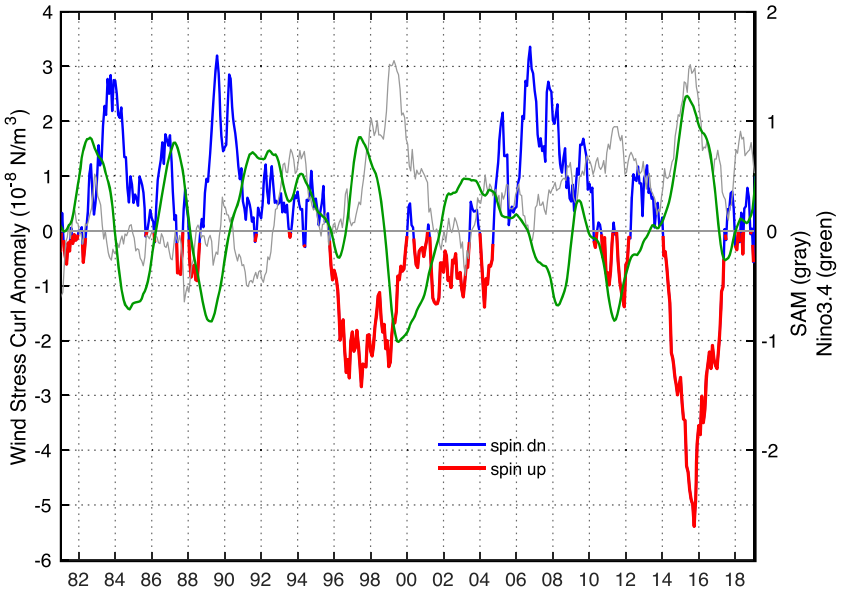

Figure 4. Wind stress curl anomaly averaged over a portion of the Weddell Gyre computed from ERA-Interim wind stress; SAM and Nino3.4 indices. The 25-month running average applied to all three time series. Wind stress curl anomaly was averaged over the region 30°W–30°E, 60–70°S.

The gyre spin up is expected to affect the export of Weddell Sea water masses into the Scotia Sea through the Orkney Passage, with a topographic sill depth of ~3,600 m (Meredith et al., 2011). Abrahamsen et al. (2019, their Figure 4) show that the current meter array within the Orkney Passage from 2011 to 2017 recorded a decrease of northward flow of Lower Weddell Sea Deep Water through the passage from early 2015 into mid-2016 to less than 2 Sv compared to ~2.5 Sv for 2013–2014. This is a likely consequence of the decrease of the sea water density at the sill depth induced by the Weddell Gyre spin-up, thus inhibiting its ability to overflow into the Scotia Sea (Meredith et al., 2008, 2011).

The Weddell Gyre spin-up may have affected the sea ice cover. A major anomaly during 2015–2017 reported in the literature is the occurrence of larger, more persistent polynya in the vicinity of Maud Rise (the Maud Rise Polynya, Cheon & Gordon, 2019; Campbell et al., 2019; Jena et al., 2019; Francis et al., 2019). The Maud Rise Polynya may be associated with stronger wind mixing, air-sea fluxes, and increased ocean eddy activity induced by the currents over the Maud Rise, which enhances local upwelling. The 2017 Maud Rise Polynya did not trigger the much larger, winter long, Weddell Polynya as it did in the mid-1970s, as the regional surface salinity in 2016–2017 was relatively low, a consequence of the +SAM, in contrast to the earlier period of prolonged −SAM (Cheon & Gordon, 2019; Gordon et al., 2007). Lee et al. (2019) conclude that the recent decrease in sea ice cover coincides with a southward expansion of the Southern Hemispheric subtropical highs (which is a marker of +SAM).

4. Conclusions

We suggest that the observed 2015–2017 freshening of the WSBW is a response to intensification of the Weddell Gyre WBC, which is driven by increased cyclonic wind stress curl over the Weddell Gyre larger-scale system, the strongest since 1982. The WSBW characteristics are expected to spread by advection and mixing to eventually reach into the AABW forming the lower limb of the Southern Ocean Meridional Overturning Circulation. For example, the deep water formed during the Weddell Polynya of the mid-1970s was observed spreading into to the Argentine Basin in 1988–1989 (Cole et al., 1996).

Another consequence of the spin-up of the Weddell Gyre may be more frequent episodes of the Maud Rise Polynya, though not of the more expansive winter long Weddell Polynya, which is more likely to form after periods of prolonged −SAM (Gordon et al., 2007).

Global climate change projects a trend toward more frequent periods of +SAM, which is associated with increased cyclonic wind stress curl over the Weddell Gyre (De Lavergne et al., 2014). We speculate that more frequent +SAM will alter the recipe of WSBW affecting the freshwater and heat inventory of the Southern Ocean Meridional Overturning Circulation.

Acknowledgments
This work was supported by NOAA's Climate Program Office's Ocean Observing and Monitoring Division (Fund Ref 100007298). Lamont-Doherty Earth Observatory contribution number 8378. All mooring data used in the paper and those CTD data not available elsewhere are available without restriction from the Columbia University Academic Commons (https://academiccommons.columbia.edu/) using the DOI indicated in the references (Huber & Gordon, 1999). See supporting information Table S1 for complete information on individual CTD stations plotted in Figure 3a. EPA was supported by Natural Environment Research Council grant NE/N018095/1 (Ocean Regulation of Climate by Heat and Carbon Sequestration and Transports, ORCHESTRA). The multiple mooring deployments and recoveries that produced the data set presented here were made possible through the generous support of several research vessel operating groups. We gratefully acknowledge the operators, officers, crew, and support staff of the Laurence M. Gould and Nathaniel B Palmer (USAP), the Ary Rongel (Brazil, NAPOC), RRS Ernest Shackleton, and RRS James Clark Ross (British Antarctic Survey). We also acknowledge Keith Nicholls of the British Antarctic Survey for his role in nurturing the cooperative arrangement between BAS and LDEO that continues to provide opportunities to maintain the Weddell mooring array.

References

Abrahamsen, E. P., Meijers, A. J. S., Polzin, K. L., Naveira Garabato, A. C., King, B. A., Firing, Y. L., et al. (2019). Stabilization of dense Antarctic water supply to the Atlantic Ocean overturning circulation. *Nature Climate Change*, *9*(10), 742–746. https://doi.org/10.1038/s41558-019-0561-2

Armitage, T. W. K., Kwok, R., Thompson, A. F., & Cunningham, G. (2018). Dynamic topography and sea level anomalies of the Southern Ocean: Variability and teleconnections. *Journal of Geophysical Research: Oceans*, *123*, 613–630. https://doi.org/10.1002/2017JC013534

Arndt, J. E., Schenke, H. W., Jakobsson, M., Nitsche, F. O., Buys, G., Goleby, B., et al. (2013). The International Bathymetric Chart of the Southern Ocean (IBCSO) version 1.0—A new bathymetric compilation covering circum-Antarctic waters. *Geophysical Research Letters*, *40*, 3111–3117. https://doi.org/10.1002/grl.50413

Campbell, E. C., Wilson, E. A., Moore, G. W. K., Riser, S. C., Brayton, C. E., Mazloff, M. R., & Talley, L. D. (2019). Antarctic offshore polynyas linked to Southern Hemisphere climate anomalies. *Nature*, *570*(7761), 319–325. https://doi.org/10.1038/s41586-019-1294-0

Carmack, E. C., & Foster, T. D. (1975). On the flow of water out of the Weddell Sea. *Deep-Sea Research*, *22*(11), 711–724. https://doi.org/10.1016/0011-7471(75)90077-7

Cheon, W. G., & Gordon, A. L. (2019). Open-ocean polynyas and deep convection in the Southern Ocean. *Scientific Reports*, *9*(1), 6935. https://doi.org/10.1038/s41598-019-43466-2

Cole, V., McCartney, M. S., Olson, D. B., & Smethie, W. M. (1996). Changes in Antarctic Bottom Water properties in the western South Atlantic in the late 1980s. *Journal of Geophysical Research*, *101*, 8957–8970. https://doi.org/10.1029/95JC03721

De Lavergne, C., Palter, J. B., Galbraith, E. D., Bernardello, R., & Marinov, I. (2014). Cessation of Southern Ocean deep convection under anthropogenic climate change. *Nature Climate Change*, *4*, 278–282. https://doi.org/10.1038/nclimate2132

Dee, D. P., Uppala, S. M., Simmons, A. J., Berrisford, P., Poli, P., Kobayashi, S., et al. (2011). The ERA-Interim reanalysis: Configuration and performance of the data assimilation system. *Quarterly Journal of the Royal Meteorological Society*, *137*(656), 553–597. https://doi.org/10.1002/qj.828

Foster, T. D., & Carmack, E. C. (1976). Frontal zone mixing and Antarctic Bottom Water formation in the southern Weddell Sea. *Deep Sea Research*, *2*, 301–317. https://doi.org/10.1016/0011-7471(76)90872-X

Francis, D., Eayrs, C., Cuesta, J., & Holland, D. (2019). Polar cyclones at the origin of the reoccurrence of the Maud Rise Polynya in austral winter 2017. *Journal of Geophysical Research: Atmospheres*, *124*, 5251–5267. https://doi.org/10.1029/2019JD030618

Fusco, G., Cotroneo, Y., & Aulicino, G. (2018). Different behaviours of the Ross and Weddell Seas surface heat fluxes in the period 1972–2015. *Climate*, *6*(1), 17. https://doi.org/10.3390/cli6010017

Gill, A. E. (1973). Circulation and bottom water production in the Weddell Sea. *Deep Sea Research and Oceanographic Abstracts*, *20*, 111–140. https://doi.org/10.1016/0011-7471(73)90048-X

Gordon, A. L. (1998). Western Weddell Sea thermohaline stratification. In S. S. Jacobs & R. Weiss (Eds.), *Ocean, ice and atmosphere interactions at the Antarctic continental margin*, *Antarctic Research Series* (Vol. 75, pp. 215–240). Washington, DC: American Geophysical Union. https://doi.org/10.1029/AR075p0215

Gordon, A. L., Huber, B., Hellmer, H., & Ffield, A. (1993). Deep and bottom water of the Weddell Sea's western rim. *Science*, *262*(5130), 95–97. https://doi.org/10.1126/science.262.5130.95

Gordon, A. L., Huber, B. A., McKee, D., & Visbeck, M. H. (2010). A seasonal cycle in the export of bottom water from the Weddell Sea. *Nature Geoscience*, *3*(8), 551–556. https://doi.org/10.1038/ngeo916

Gordon, A. L., Visbeck, M., & Comiso, J. C. (2007). A possible link between the Weddell Polynya and the Southern Annular Mode. *Journal of Climate*, *20*(11), 2558–2571. https://doi.org/10.1175/JCLI4046.1

Gordon, A. L., Visbeck, M., & Huber, B. (2001). Export of Weddell Sea deep and bottom water. *Journal of Geophysical Research*, *106*, 9005–9017. https://doi.org/10.1029/2000jc000281

Huber, B. A., & Gordon, A. L. (1999-2019). *Temperature-salinity data from mooring M3, northwest Weddell Sea*. New York, NY: Columbia University Academic Commons. https://doi.org/10.7916/d8-801t-yg44

Jacobs, S. S. (1991). On the nature and significance of the Antarctic slope front. *Marine Chemistry*, *35*, 9–24.

Jena, B., Ravichandran, M., & Turner, J. (2019). Recent reoccurrence of large open-ocean polynya on the Maud Rise seamount. *Geophysical Research Letters*, *46*, 4320–4329. https://doi.org/10.1029/2018GL081482

Lee, S.-K., Volkov, D., Lopez, H., Cheon, W. G., & Gordon, A. L. (2019). *The record-low Antarctic sea-ice extent in 2017 and the associated atmosphere-ocean processes*. Montreal: IUGG.

Legg, S., Chang, Y., Chassignet, E., Danabasoglu, G., Ezer, T., Gordon, A., et al. (2009). Improving oceanic overflow representation in climate models: The gravity current entrainment climate process team. *Bulletin of the American Meteorological Society*, *90*(5), 657–670. https://doi.org/10.1175/2008BAMS2667.1

Marshall, J., & Speer, K. (2012). Closure of the meridional overturning circulation through Southern Ocean upwelling. *Nature Geoscience*, *5*, 171–180. https://doi.org/10.1038/ngeo1391

McKee, D., Yuan, X., Gordon, A. L., Huber, B. A., & Dong, Z. (2011). Climate impact on interannual variability of Weddell Sea bottom water. *Journal of Geophysical Research*, *116*, C05020. https://doi.org/10.1029/2010JC006484

Meijers, A. J. S., Cerovečki, I., King, B. A., & Tamsitt, V. (2019). A see-saw in Pacific subantarctic mode water formation driven by atmospheric modes. *Geophysical Research Letters*, *46*, 13,152–13,160. https://doi.org/10.1029/2019GL085280

Meijers, A. J. S., Meredith, M. P., Abrahamsen, E. P., Morales Maqueda, M. A., Jones, D. C., & Naveira Garabato, A. C. (2016). Wind-driven export of Weddell Sea slope water. *Journal of Geophysical Research, Oceans*, *121*, 7530–7546. https://doi.org/10.1002/2016JC011757

Meredith, M. P., Gordon, A. L., Naveira Garabato, A. C., Abrahamsen, E. P., Huber, B. A., Jullion, L., & Venables, H. J. (2011). Synchronous intensification and warming of Antarctic bottom water outflow from the Weddell gyre. *Geophysical Research Letters*, *38*, L03603. https://doi.org/10.1029/2010GL046265

Meredith, M. P., Naveira Garabato, A. C., Gordon, A. L., & Johnson, G. C. (2008). Evolution of the deep and bottom waters of the Scotia Sea, Southern Ocean, during 1995–2005. *Journal of Climate*, *21*(13), 3327–3343. https://doi.org/10.1175/2007JCLI2238.1

Muench, R., & Gordon, A. L. (1995). Circulation and transport of water along the western Weddell Sea margin. *Journal of Geophysical Research*, *100*, 18,503–18,515. https://doi.org/10.1029/95JC00965

Orsi, A. H., Jacobs, S. S., Gordon, A. L., & Visbeck, M. (2001). Cooling and ventilating the abyssal ocean. *Geophysical Research Letters*, *28*, 2923–2926. https://doi.org/10.1029/2001GL012830

Orsi, A. H., Johnson, G. C., & Bullister, J. L. (1999). Circulation, mixing and production of Antarctic bottom water. *Progress in Oceanography*, *43*(1), 55–109. https://doi.org/10.1016/S0079-6611(99)00004-X

Orsi, A. H., Smethie, W. M., & Bullister, J. L. (2002). On the total input of Antarctic waters to the deep ocean: A preliminary estimate from chlorofluorocarbon measurements. *Journal of Geophysical Research*, *107*, 3122. https://doi.org/10.1029/2001JC000976

Purkey, S. G., & Johnson, G. C. (2013). Antarctic bottom water warming and freshening: Contributions to sea level rise, ocean freshwater budgets, and global heat gain. *Journal of Climate*, *26*(16), 6105–6122. https://doi.org/10.1175/JCLI-D-12-00834.1

Purkey, S. G., Smethie, W. M. Jr., Gebbie, G., Gordon, A. L., Sonnerup, R. E., Warner, M. J., & Bullister, J. L. (2018). A synoptic view of the ventilation and circulation of Antarctic bottom water from chlorofluorocarbons and natural tracers. *Annual Review of Marine Science*, *10*(1), 503–527. https://doi.org/10.1146/annurev-marine-121916-063414

Stewart, A. L., & Thompson, A. F. (2013). Connecting Antarctic cross-slope exchange with Southern Ocean overturning. *Journal of Physical Oceanography*, *43*(7), 1453–1471. https://doi.org/10.1175/JPO-D-12-0205.1

Su, Z., Stewart, A. L., & Thompson, A. F. (2014). An idealized model of Weddell gyre export variability. *Journal of Physical Oceanography*, *44*(6), 1671–1688. https://doi.org/10.1175/JPO-D-13-0263.1

Vernet, M., Geibert, W., Hoppema, M., Brown, P. J., Haas, C., Hellmer, H. H., et al. (2019). The Weddell Gyre, Southern Ocean: Present knowledge and future challenges. *Reviews of Geophysics*, *57*(3), 623–708. https://doi.org/10.1029/2018RG000604

Yuan, X. (2004). ENSO-related impacts on Antarctic sea ice: A synthesis of phenomenon and mechanisms. *Antarctic Science*, *16*, 415–425. https://doi.org/10.1017/S0954102004002238

Yuan, X., Kaplan, M. R., & Cane, M. A. (2018). The interconnected global climate system—A review of tropical–polar teleconnections. *Journal of Climate*, *31*, 5765–5792. https://doi.org/10.1175/JCLI-D-16-0637.1